

# Shot noise in generic quantum dots: crossover from ballistic to diffusive transport

H.-S. Sim and H. Schomerus

Max-Planck-Institut für Physik komplexer Systeme, Nöthnitzer Str. 38, 01187 Dresden, Germany

**Abstract.** We study shot noise for generic quantum dots coupled to two leads and allow for an arbitrary strength of diffractive impurity scattering inside the dots. The ballistic quantum dots possess a mixed classical phase space, where regular and chaotic regions coexist. In absence of disorder, the noise is systematically suppressed below the universal value of fully chaotic systems, by an amount which varies with the positions of the leads. This suppression is due to the deterministic nature of transport through regular regions and along short chaotic trajectories, and disappears by increasing the scattering rate, which is incorporated by using the Poisson kernel of random matrix theory.

## 1. Introduction

The discreteness of the electron charge  $e$  causes time-dependent current fluctuations even at zero temperature. These fluctuations are known as shot noise and recently have received much attention in mesoscopic physics (for a review see [1]). One prominent class of mesoscopic systems are classically chaotic ballistic cavities (quantum dots). For incoherent transport through a chaotic quantum dot coupled to two leads, each having  $N$  channels, the shot noise would assume the Poissonian value  $P_0 = 2eG_0V$ , where  $G_0 = Ne^2/(2h)$  and  $V$  is the voltage difference between the leads. For low temperatures, correlations of electrons due to Fermi statistics suppress the noise  $P$  by a factor of  $F = P/P_0$  relative to the value  $P_0$  of uncorrelated electrons. In chaotic quantum dots, the suppression factor  $F = F_{\text{ch}} = 1/4$  has been found to be universal, i.e., independent of the details of systems, by using random matrix theory [2, 3] and semiclassical methods [4], which has been confirmed by an experiment [5]. The origin of the low-temperature noise in chaotic quantum dots is the *probabilistic* nature of quantum transport: Each attempt to transmit a charge  $e$  through the system succeeds with a finite probability.

Very recently, further reductions of shot noise below  $F_{\text{ch}}$  due to residual signatures of classically *deterministic* scattering have been discussed by Agam, Aleiner, and Larkin [6]. This non-universal suppression of the noise appears when the dwell time of electrons is smaller than the time scale of quantum diffraction (the Ehrenfest time in chaotic systems). This has also been verified in a recent experiment [7].

Generic ballistic quantum dots are not fully chaotic but possess a mixed classical phase space [8], where regular islands are separated from chaotic seas by impenetrable dynamical barriers. Signatures of the mixed phase space in quantum transport have been found in the conductance, which exhibits fractal fluctuations [9] and isolated resonances [10, 11]. In this proceeding paper, we address the effect of the mixed phase space and of disorder on the shot-noise suppression.

We study shot noise for generic quantum dots coupled to two leads, with varying the positions and the widths of the leads, and allow for an arbitrary strength of elastic diffractive

impurity scattering inside the dots. In Ref. [12] this combination of effects was used to investigate the time scales of deterministic transport through the quantum dots. In the present paper we concentrate on the effect of impurity scattering itself. In absence of impurity scattering, the suppression factor  $F$  is systematically reduced below the universal value  $F_{\text{ch}}$  of fully chaotic systems, by an amount which varies with the parameters (positions and widths) of the attached leads. This reduction of  $F$  is not only due to the deterministic nature of transport along short chaotic trajectories, but also because quantum diffraction is strongly reduced for transport through regular regions, as well, thus, the dependence of  $F$  on the parameters of leads can be understood from the fact that the amount of deterministic processes coupled to the leads varies with the parameters. This feature becomes clarified after adding diffractive impurity scattering with the aid of the Poisson kernel [3, 13, 14, 15] of random matrix theory. As the rate of diffractive scattering increases, the suppression factor  $F$  becomes larger and eventually recovers the universal value  $F_{\text{ch}}$  of fully chaotic systems.

In our numerical simulation, the annular billiard [16] is chosen as a model of a ballistic quantum cavity with mixed phase space. We will discuss the classical motion in the billiard in Sec. 2, and incorporate diffractive scattering in Sec. 3. In Sec. 4, the dependence of  $F$  on the parameters of the leads will be discussed in absence and presence of diffractive scatterings, and the role of regular versus chaotic classical motion on shot noise will be clarified. In Sec. 5, finally, some concluding remarks will be given.

## 2. Annular billiards

An exemplary model for mixed regular and chaotic classical dynamics is the two-dimensional annular billiard [16], which consists of the region between two circles with radii  $R$ ,  $r$ , and eccentricity  $e$ . Its schematic diagram is drawn in Fig. 1(a). To study shot noise, two leads (openings) of width  $W$  are attached opposite to each other at an angle  $2\theta \in [0; \pi]$  with respect to the axis through the two circle centers. Two values of  $W$  are selected as  $W = 0.222R$  and  $W = 0.347R$ ; the former corresponds to leads with six channels, while the latter to ten channels. The other parameters of  $r$  and  $e$  are fixed as  $r = 0.6R$  and  $e = 0.22R$ , respectively, in terms of  $R$  throughout this work.

### 2.1. Classical motion in annular billiards

The classical phase space of the annular billiard can be parameterized by the impact parameter  $s$  and the transverse component of the momentum  $\sin\theta$  (with  $\theta$  the angle of incidence) of trajectories that are reflected at the exterior circle. The phase space of the closed annular billiard is shown in Fig. 1(b), which displays two regular whispering-gallery regions, a large regular island, neighboring satellite islands, and a chaotic sea. Figs. 1(c) and (d) show the phase space of the open annular billiard (with opening width  $W = 0.222R$ ), which only includes trajectories of particles that are injected into the billiard through leads attached at  $\theta = 0$  and  $\theta = \pi/2$ , respectively. The large island is well coupled to one of the openings for  $\theta = 0$ , and is completely decoupled from both openings at  $\theta = \pi/2$  [see the empty region at the center of Fig. 1(d)]. The chaotic sea and whispering-gallery regions are well coupled for arbitrary position of the openings, while the coupling of the satellite islands depends on  $\theta$  and  $W$ . In this way one can select regions in phase space by varying  $\theta$  and  $W$ .

In the open billiard some classical trajectories entering into the chaotic sea escape without many billiard-boundary scatterings so that the chaotic sea appears less chaotic than in the closed billiard. One can see this modification of phase space, e.g., near  $s = 0$  in Fig. 1(c) and around the empty center in (d). The role of these short chaotic trajectories on shot noise will be discussed later.

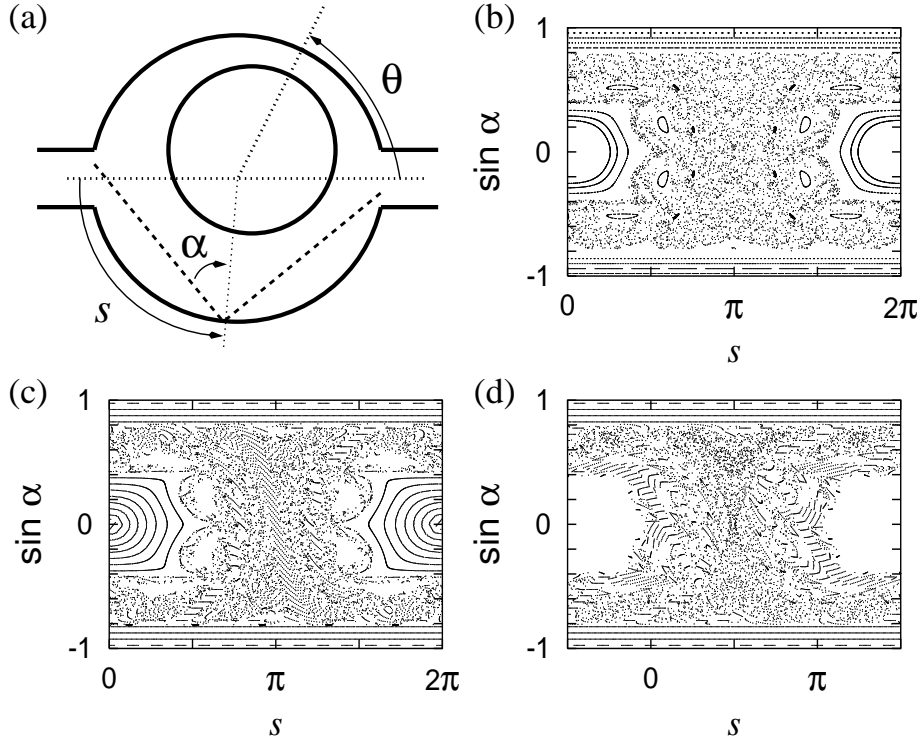


**Figure 1.** (a) Schematic diagram of the annular billiard between two circular hard walls of exterior radius  $R$ , interior radius  $r = 0.6R$ , and eccentricity  $e = 0.22R$ . Two openings of width  $W = 0.222R$  are attached opposite to each other at an angle  $2\theta \in [0; \pi]$  relative to the line connecting the circle centers. (b) Phase space, parameterized by the impact parameter  $s$  and the transverse momentum component  $\sin \alpha$  of trajectories at the exterior circle. The lower panels show the phase space for open billiards with  $\theta = 0$  (c) and  $\theta = \pi/2$  (d), for which we only record trajectories that are injected through the openings (until they leave the billiard again).

## 2.2. Conductance and shot noise formula

We calculated the dimensionless conductance  $T$  and the shot-noise suppression factor  $F$  from the relations [1],

$$T = \text{tr} t^y t; \quad (1)$$

$$F = (2N)^{-1} \text{tr} t^y t (1 - t^y t); \quad (2)$$

Here,  $N$  is the number of channels in each lead and the transmission matrix  $t$  is a subblock of the scattering matrix

$$S = \begin{pmatrix} r & t^0 \\ t & r^0 \end{pmatrix}; \quad (3)$$

where  $r$  and  $r^0$  are reflection coefficients and the transmission matrix  $t^0$  contains the same information as  $t$ . The scattering matrix is obtained numerically by the method of recursive Green functions [17], for which space is discretized on a square lattice. In terms of the lattice constant  $a$ , we choose  $R = 144a$ ,  $r = 86.4a$ , and  $e = 31.7a$ . Energy  $E$  will be measured in units of  $\hbar^2/(2m a^2)$  and time in units of  $2m a^2/\hbar$ , with  $m$  the mass of the charge carriers. In these units the mean level spacing is estimated as  $\Delta = 4/\mathcal{A} \approx 0.003$ , where  $\mathcal{A} = (R^2 - r^2)/a^2$  is the dimensionless area of billiard. We will work in the energy

window  $E \in (0.408; 0.433)$ . In this window, the Fermi wavelength  $\lambda_F \approx 9.5a$ , resulting in  $N = \text{Int}(2W/\lambda_F) = 6$  for  $W = 0.222R = 32a$  and  $N = 10$  for  $W = 0.347R = 50a$ .

### 3. Elastic diffractive scatterings

We now introduce elastic diffractive scatterings with the aid of the Poisson kernel [13, 14, 15], a statistical ensemble of random matrix theory [3]. In the Poisson kernel one averages the scattering matrix over an energy range  $E_{av}$ , in this way eliminating the system-specific details of the dynamics with time scales longer than  $\tau_{av} = \hbar/E_{av}$ , and replaces these by random dynamics of the same universality class as elastic diffractive impurity scattering. The effective mean free scattering time  $\tau_{av}$  can be tuned by changing the energy-averaging window  $E_{av}$ .

In our numerical simulation, the elimination of the system-specific details on time scales larger than  $\tau_{av}$  is achieved by averaging the scattering matrix  $S$  over an energy range  $[E_0 - E_{av}/2; E_0 + E_{av}/2]$  of width  $E_{av} = \hbar/\tau_{av}$  (which will be taken inside the total energy range  $[0.408, 0.433]$  of our numerical simulation),

$$\overline{S}(E_{av}; E_0) = \frac{1}{E_{av}} \int_{E_0 - E_{av}/2}^{E_0 + E_{av}/2} dE S(E) : \quad (4)$$

Here the information on processes with longer time scales than  $\tau_{av}$  is lost, because it is encoded into the short-range energy correlations (fluctuations) of the scattering matrix, while the information on the dynamics on shorter time scales than  $\tau_{av}$  modulates the scattering matrix on larger energy scales and hence is retained. Diffusive motion then is introduced by coupling to an auxiliary system with scattering matrix  $S_0$  taken from the appropriate circular ensemble of random matrix theory (observing the same symmetries as the original scattering matrix, as time-reversal or spatial parities [18]), resulting in

$$S^0(E_{av}; E_0; S_0) = \overline{S}(E_{av}; E_0) + T^0(1 - S_0 R)^{-1} S_0 T : \quad (5)$$

The ensemble of scattering matrices (5) is the so-called Poisson kernel [3, 13, 14, 15], with  $\overline{S}$  the so-called optical scattering matrix. The coupling matrices  $T$ ,  $T^0$ , and  $R$  must be chosen such that  $S^0$  is a unitary matrix, but the invariance of the circular ensemble guarantees that results do not depend on their specific choice.

Then, the mean suppression factor  $F(E_{av})$  (or the conductance  $T$ ) can be obtained for fixed  $E_{av}$  (and hence fixed  $\tau_{av}$ ), first by averaging the noise (or the conductance) within each Poisson kernel (fixing also  $E_0$ ), and then averaging these values over  $E_0 \in (0.408; 0.433)$ .

## 4. Results and discussions

### 4.1. Absence of diffractive scatterings: the dependence of shot noise on the positions and on the widths of the leads

The energy-averaged conductance  $T$  and the energy-averaged suppression factor  $F$  in the window of  $E \in (0.408; 0.433)$  are shown as the values at  $E_{av} = 0$  of Figs. 2 and 3 for different  $\alpha$  and  $W$ . Our first observation for the shot noise is that for all values of  $\alpha$ , the suppression factor is smaller than the universal value  $1/4$  of fully chaotic motion. Moreover, the shot noise is more suppressed for the cases that one opening couples to the large regular island ( $0 < \alpha < 0.3$ ) than for the cases in which the regular islands is decoupled from the openings ( $\alpha > 0.4$ ). This behavior indicates that electrons injected into the large regular island contribute less to the shot noise, which will be clarified in the analysis incorporating diffractive scatterings in Sec. 4.2.

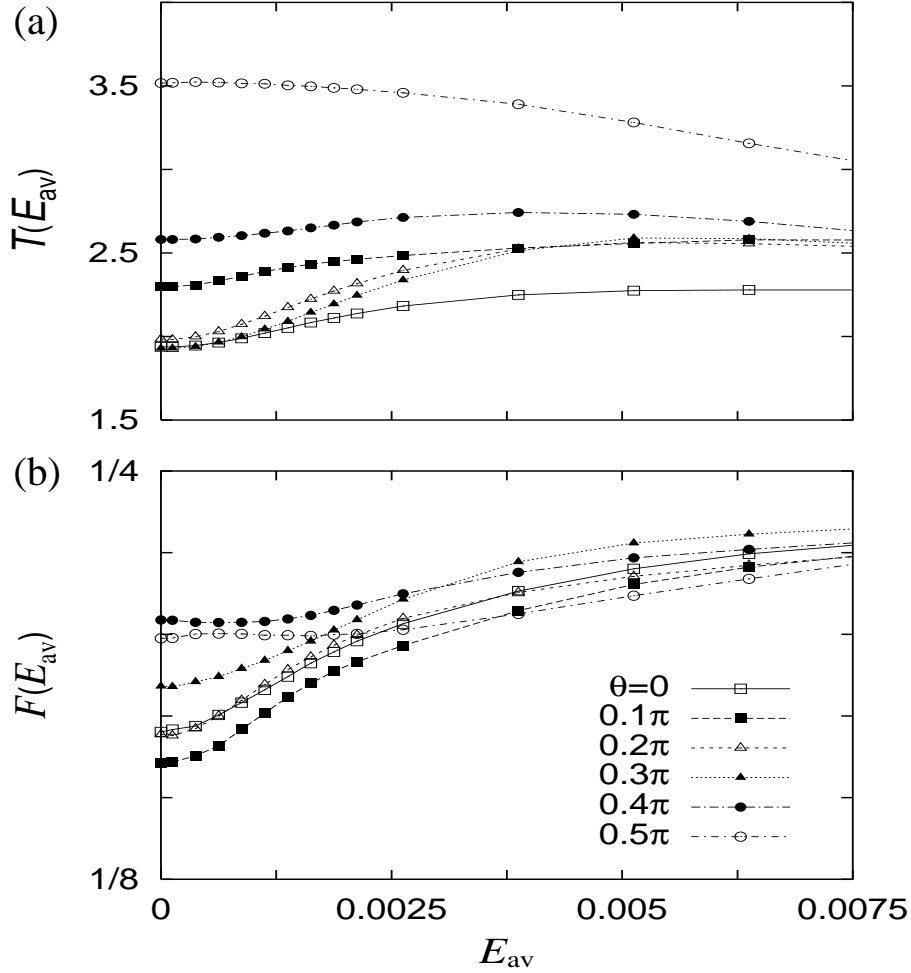


**Figure 2.** (a) Transmission  $T$  and (b) shot-noise suppression factor  $F$  (lower panel) as a function of the strength of diffractive impurity scattering with a rate  $\Gamma = E_{av}/\hbar$ , for different positions  $\theta$  of the leads with  $W = 0.222R$  ( $N = 6$ ). In (a), the same symbols are used for each  $\theta$  as in (b).

The suppression factors are strongly reduced for  $W = 0.347R$  than for  $W = 0.222R$ , as shown in Figs. 2 and 3. This feature will be also understood in Sec. 4.2 from the fact that the amount (per channel in the leads) of deterministic trajectories, which include those in the regular islands and those escaping the dots without many billiard-boundary scatterings in the chaotic sea, increases for the leads with broader widths.

We note that the dependence of conductance  $T$  on  $\theta$  shows a similar features to that of the suppression factor; conductance is smaller for the well-coupled cases to the regular islands ( $0 < \theta < 0.3$ ) than for the decoupled cases ( $\theta > 0.4$ ). This behavior can be understood from the fact that for  $0 < \theta < 0.3$  the regular island is well coupled only to one opening, so that electrons entering the regular island do not contribute to transmission. This similarity, however, is accidental. As will be demonstrated in Sec. 4.2, deterministic processes will always suppress shot noise (when their area in phase space is larger than a Planck cell, so that they are well resolved), while they enhance or suppress conductance, depending on the shape of the quantum dot and the positions of the leads.

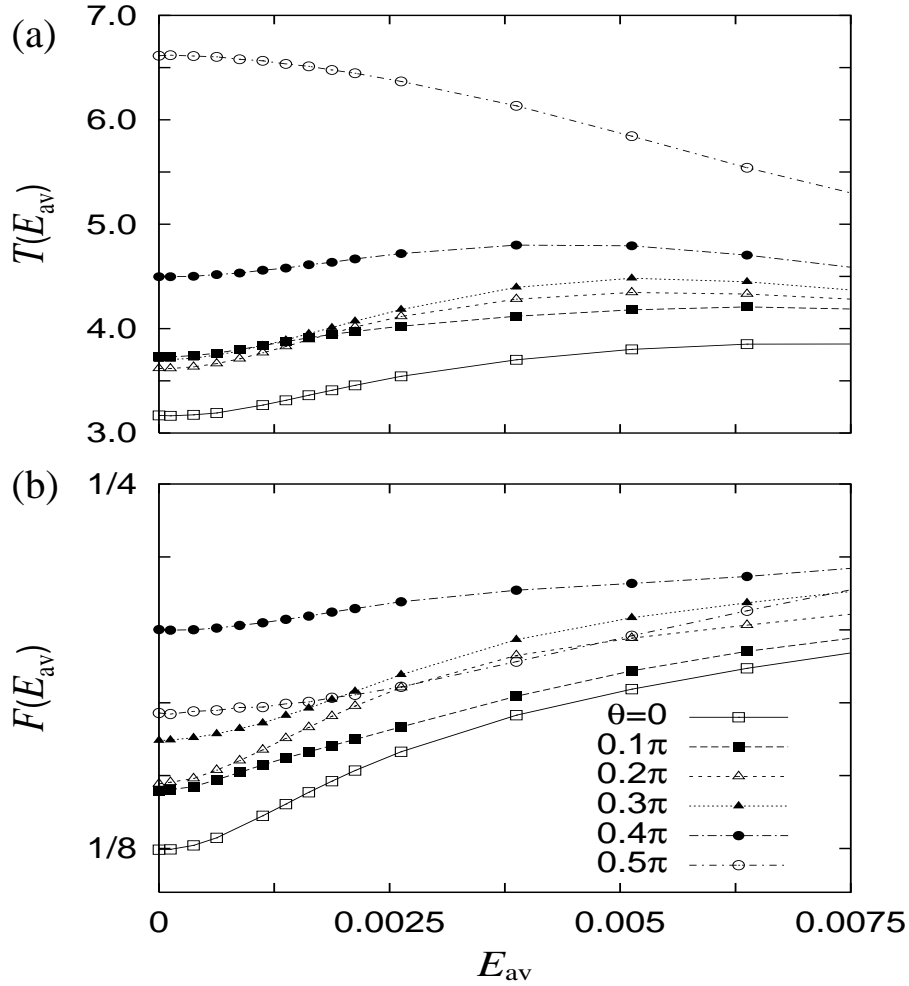


**Figure 3.** The same as Fig. 2, but for  $W = 0.347R$  ( $N = 10$ ).

#### 4.2. Role of regular versus chaotic classical motion in shot-noise suppression

The effect of the diffractive scattering on the conductance  $T$  and the shot-noise suppression factor  $F$  for different positions of the leads are shown in Figs. 2 and 3.

The values of  $T$  and  $F$  at  $E_{av} = 0$  are those in absence of diffractive impurity scattering, because the Poisson kernel becomes a delta function at  $S(E_0)$  as  $\bar{S}$  approaches this unitary matrix for  $E_{av} \rightarrow 0$ . For increasing  $E_{av}$ ,  $T(E_{av})$  and  $F(E_{av})$  approach their universal values of random-matrix theory, because  $\bar{S} = 0$  in this limit. Note that spatial symmetries such as up-down and left-right reflections affect the weak localization corrections to the universal values [18]. The correction is enhanced (absent) for  $\theta = 0 (0.5\pi)$ , where there is up-down (left-right) reflection symmetry [18], compared with the other values of  $\theta$  with no spatial symmetry.

The function  $F(E_{av})$  is monotonically increasing almost everywhere (negative values of the slope are within the statistical uncertainty in the numerical simulation), indicating that the noise is *enhanced* when the system-specific deterministic details of the transport are replaced by the indeterministic transport of random matrix theory. Consequentially, one can define the probability distribution of deterministic processes with dwell time  $\tau_{dwell} \rightarrow \tau_{av}$  by the rate of change of the shot-noise suppression  $F(E_{av})$  which can be substantiated by a semiclassical

analysis [12].

The crossover of shot noise from ballistic to diffusive transport occurs at different scattering rate  $\hbar=E_{av}$ , depending on  $\alpha$  and  $W$ . We will discuss first for the case of  $W = 0.222R$ . In the three cases  $\alpha = 0, 0.1, 0.2$ , in which the leads couple to the large regular island in phase space, the crossover occurs already at very small  $E_{av}$ , while it starts above an energy  $E_{indet} = 0.002$  for  $\alpha = 0.4, 0.5$  (where the regular region is decoupled). The former is due to the deterministic processes of very long dwell times in the large regular island, which can be affected by diffractive scatterings of very small scattering rate. On the other hand, the latter is due to the fact that the processes in the chaotic sea are already indeterministic for times larger than  $\hbar=E_{indet}$ , which can be interpreted as the Ehrenfest time.

For the leads with larger width  $W$ , more deterministic processes of regular regions can couple to the leads and more short deterministic trajectories in the chaotic sea appear. This feature entails that for the leads with  $W = 0.347R$  (Fig. 3),  $F(E_{av})$  approaches to  $F_{ch}$  more slowly than for the case of  $W = 0.222R$  (Fig. 2). Similarly, for the leads at  $\alpha = 0.5$  and with  $W = 0.347R$  the suppression factor  $F(E_{av})$  starts to increase at earlier  $E_{av}$  than  $E_{indet}$  (which is obtained in the curves for  $W = 0.222R$ ), since small regular islands additionally couple to the leads with  $W = 0.347R$ .

We note that in contrast to  $F(E_{av})$ , the sign of the slope of  $T(E_{av})$  depends on the system-specific geometry, e.g., on lead position [see Figs. 2(a) and 3(a)]. This shows that conductance can be either enhanced or suppressed by diffractive scattering (indeterministic processes).

## 5. Concluding remarks

The shot noise reduction due to deterministic transport suggests that shot noise can be used as a probe of classical phase space of generic quantum dots (conductance can not be used as such a probe). The crossover of shot noise from ballistic to diffusive transport, shown in Figs. 2(b) and 3(b), could be probed experimentally by measuring shot noise while tuning the disorder strength, which can be achieved by adjusting a gate voltage [19].

## References

- [1] Blanter Ya M and Büttiker M 2000 Phys. Rep. **336** 1-166
- [2] Jalabert R A et al 1994 Europhys. Lett. **27** 255-260
- [3] Beenakker C W J 1997 Rev. Mod. Phys. **69** 731-808
- [4] Blanter Ya M and Sukhorukov E V 2000 Phys. Rev. Lett. **84** 1280-1283
- [5] Oberholzer S et al 2001 Phys. Rev. Lett. **86** 2114-2117
- [6] Agam O et al 2000 Phys. Rev. Lett. **85** 3153-3156
- [7] Oberholzer S et al 2002 Nature **415** 765-767
- [8] Markus L and Meyer K R 1974 Memoirs of the AMS **144** (Providence: American Mathematical Society)
- [9] Ketzmerick R 1996 Phys. Rev. B **54** 10841-10844
- [10] Huckestein B et al 2000 Phys. Rev. Lett. **84** 5504-5507
- [11] Hufnagel L et al 2001 Europhys. Lett. **54** 703-708
- [12] Sim H-S and Schomerus H 2002 Phys. Rev. Lett. in press
- [13] Mello P A et al 1985 Ann. Phys. (N. Y.) **161** 254-275
- [14] Brouwer P W 1995 Phys. Rev. B **51** 16878-16884
- [15] Baranger H U and Mello P A 1996 Europhys. Lett. **33** 465-470
- [16] Bohigas O et al 1993 Nucl. Phys. A **560** 197-210
- [17] Baranger H U et al 1991 Phys. Rev. B **44** 10637-10675
- [18] Baranger H U and Mello P A 1996 Phys. Rev. B **54** 14297-14300
- [19] Toyoda E et al 1999 Phys. Rev. B **59** R11653-R11656